Design and Application of Diamond Bit Water Passage System, Seafloor Drill Parameters

Jialiang Wang (Jialiangwang2019@163.com)
Hunan University of Science and Technology https://orcid.org/0000-0002-8184-2474
Dilei Qian
Hunan University of Science and Technology
Yang Sun
Hunan University of Science and Technology
Fenfei Peng
Hunan University of Science and Technology

Original Article

Keywords: Seafloor drill, Water passage system, Diamond bit, Drilling fluid, Fluid simulation

Posted Date: June 22nd, 2021

DOI: https://doi.org/10.21203/rs.3.rs-634361/v1

Design and Application of Diamond Bit Water Passage System, Seafloor Drill Parameters

Jialiang Wang* [1 2], Dilei Qian[1 2], Yang Sun[1 2]. Fenfei Peng[1 3]

(1 National Local Joint Engineering Laboratory of Marine Mineral Resources Exploration Equipment and Safety Technology, Xiangtan 411201, China; 2. Hunan University of Science and Technology, School of Mechanical Engineering, Xiangtan 411201, China; 3. Key Laboratory of Metallogenic Prediction of Nonferrous Metals and Geological Environment Monitoring (Central South University), Ministry of Education)

Abstract: The operation and formation characteristics of a seafloor drill are utilized to design a water passage system for bottom-jetting diamond bits based on the multi-objective optimization theory. Fluid dynamics theory and the effects of bit rotation on the flow field at the hole bottom are used to analyze the impact of structural and drilling parameters of the HQ-size bit on the flow field of the waterway system. Considering the effect of the grinding length ratio of the bit on the lopsided wear of the inner and outer diameters, the water passage system parameter design and maximum projection area of the cutting tooth are effective optimization goals to improve the normal service life of the bit. The flow field of the drilling fluid at the hole bottom becomes more turbulent and the efficiency of carrying cuttings return decreases as the waterway height of the bit increases. The optimal bit rotation speed is 250-400 rpm. When drilling into conventional formations, the pump displacement should be controlled within the range of 50-80 L/min. When drilling into sediment formations, the pump displacement should be controlled within the range of 50-65 L/min. An on-site drilling test verified the rationality of the bit water passage system design and corresponding drilling parameters.

Key words: Seafloor drill; Water passage system; Diamond bit; Drilling fluid; Fluid simulation

Introduction

The seafloor is rich in mineral resources such as oil, natural gas, combustible ice, polymetallic ooze, and cobalt-rich manganese nodules [1, 2]. Mineral reserves can be evaluated to directly obtain cores from the seafloor by drilling. There are two main sampling methods used for exploring marine mineral resources: large drilling ships and seafloor drills, as shown in Figure 1 [3]. When using the large drilling ship for operation, the drilling tower is located on the deck of a mother ship. With the cooperation of the drilling tower, the drill pipes are connected to the seafloor one-by-one and the drilling process begins. After each drilling run, the coring barrel filled with the samples is lifted from the hole bottom to the mother ship through a fishing device, then a new core barrel is lowered to begin the subsequent drilling process. When using a seafloor drill, the rig and all core barrels are directly lowered to the seafloor through an armored cable as an operator controls them remotely from the mother ship. After the end of a single drilling footage, the core-filled core barrel is first lifted from the hole bottom and stored in the drilling tool library of the rig

*Corresponding author .Tel.:+86-731-13507313232;
E-mail address:Jialiangwang2019@163.com

before a new core barrel is lowered to start the next drilling process. This cycle is repeated until the drilling operation is complete and the rig is recovered to the mother ship. The operation mode of the seafloor drill, unlike those of large drilling ships, has more lax requirements for mother ship configurations and can be performed quicker; it also has higher operation efficiency. When drilling within 200 m is carried out within a water depth of 3000 m, the seafloor drill is more advantageous in terms of both performance and cost [4-6].

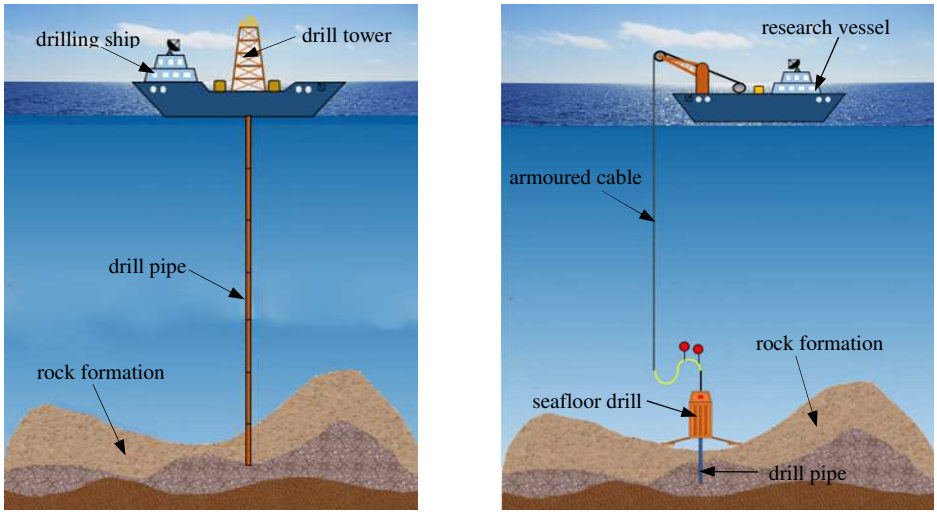

Fig. 1 Two methods of seafloor sampling

The performance of the diamond bit directly affects the drilling efficiency of seafloor drills. Sedimentary strata mixed with hard rock strata dominate the space within 200 m of the seafloor. When drilling in this type of formation, the seafloor drill can be adaptively switched in real-time between the push coring and rotary coring modes according to changes in the formation characteristics [7, 8]. Whether the design of the bit water passage system is reasonable or not directly affects the drilling efficiency and service life of the bit. Compared with the conventional diamond bit design, the diamond bit used in seafloor drills requires a more complicated water passage system design. For instance, the drilling fluid pump frequently opens and closes during the adaptive switching between push coring and rotary coring drilling modes. If the design of the bit water passage system is unreasonable, the probability of premature scrapping due to burnout and abnormal wear increases significantly. Additionally, the flow rate and head of the built-in water pump of the seafloor drill are lower than the mud pump used in a land core drilling rig; they also utilize seawater directly as the borehole drilling medium. The ability of seawater to carry cuttings, the wall protection performance, and the cooling effect on the cutting teeth of the bit are lower than those of mud drilling medium [9, 10]. Further, when drilling in sediment formations, the drilling fluid readily causes severe erosion on the hole wall and core. It is necessary to reasonably control the drilling fluid core surface velocity and return velocity as the bit water passage system is operated [11, 12].

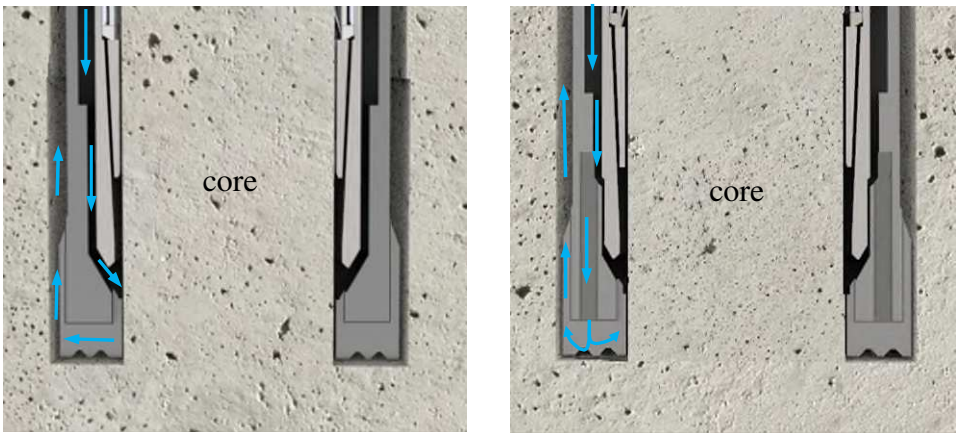

(a) Conventional diamond bit (b) Bottom jetting diamond bit

Fig. 2 Water passage system of diamond bits

Core drilling uses conventional type or bottom jetting type diamond bits depending on the differences in water passage systems, as shown in Figure 2 [13-14]. After passing through the clearance between the bit and the core lifter case, the drilling fluid of the conventional bit returns along the annulus between the hole wall and the outer diameter of the drill pipe. The primary working formation of the seafloor drill is comprised of sediments, as mentioned above. Selecting a bottom jetting bit prevents direct erosion of most drilling fluids on sediments and improves the coring recovery rate. The water passage system of the bottom jetting bit mainly includes waterways, nozzles, and internal and external water grooves. Existing bottom jetting bit water passage system designs are mainly based on engineering practice rather than systematically gathered, empirical evidence; the design process usually involves ignoring the effects of the nozzle quantity on the bottom crown area of the bit and the grinding ratio of its inner and outer diameters [15-16]. When distribution of diamonds in the matrix is uniform and the bit has rectangular waterway shape, the cutting tooth is fan-shaped. Therefore, the working load of diamonds near the inner diameter edge is significantly higher than that of the diamonds near the outer diameter edge. When drilling in complex formations, the inner diameter of the bit is more prone to wear; this renders the core unable to smoothly enter the core pipe due to its diameter, scrapping the bit in advance [17]. When the ratio of the outer diameter to the inner diameter of the bit is greater than 1.2, the risk of lopsided wear on the bit increases significantly [18]. To satisfy the working conditions of seafloor drills, it is essential to design the bit water passage system properly.

Based on the basic theory of multi-objective optimization, this paper proposes a water passage system design method that is suitable for bottom jetting bits based on seafloor drill formation and operation characteristics. The proposed method is based on fluid dynamics theory and accounts for the effects of bit rotation on the flow field at the hole bottom. The effects of the structural parameters of the water passage system and the bit drilling parameters on the

flow field at the hole bottom are analyzed. Field drilling tests were conducted to verify the rationality of the scheme. This work may enrich the existing design theory for water passage systems, improve the operational efficiency of seafloor drills in soft and hard interlaced complex formations, and help to satisfy the practical demand for lightweight and miniaturized marine resource exploration equipment.

1 Bit water passage system design

1.1 Bit water passage system structure

The seafloor drill uses wire-line coring drilling technology, so the cutting teeth of the bit matched with the rig have a relatively thick wall. The bit water passage system was designed with main waterways and assistant waterways to enhance the cooling effect of the drilling fluid on its cutting teeth and to control the grinding ratio of its inner and outer diameters, thus preventing lopsided wear. Nozzles are set in the main waterways and the assistant waterways. The assistant waterways arranged on the cutting teeth of the bit are not completely penetrated along the inner diameter direction, which ensures an effective working area for the cutting teeth and reduces the likelihood of lopsided wear.

Figure 3 shows the bottom crown structure diagram of the bottom jetting bit, where r_1 and r_2 are the main and assistant nozzles radius, respectively, and d and D are the inner and outer diameter of the bit. For the sake of convenient manufacturing, a rectangular nozzle is adopted. The width of the inner and outer water groove is equal to the width of the waterway. The width of the main waterway b_1 is 2 (r_1+1) and that of the assistant waterway b_2 is 2 (r_2+1).

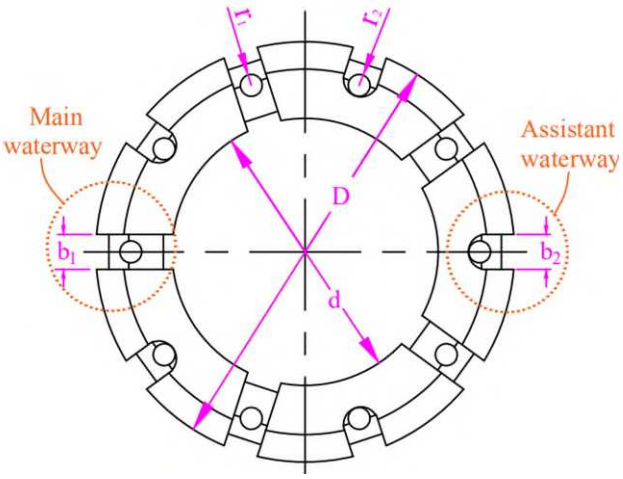

Fig. 3 Bottom crown structure of bit

1.2 Design principle and water passage system parameters of bit

Most of the bottom jetting bit flows return along the outside annulus after flowing through the nozzles; only a small portion of the drilling fluid passes through the water clearance between the core lifter case and the rigid body of

the bit. Therefore, the flow rate generated from the water clearance on the flow rate of the outside annulus can be ignored. According to the law of mass conservation, the total flow rate of the drilling fluid flowing through the nozzles is equal to the flow rate flowing through the outside annulus, that is, the product of the average velocity of the cross-section flowing through and the cross-sectional area. This can be expressed as follows:

$$V_2 S_T = V_1 \frac{\pi}{4}(D_1^2 - D_2^2) \tag{1}$$

where S_T is the total water passing area of the nozzles, D_1 is the diameter of the hole wall, D_2 is the outer diameter of the drill pipe, V_1 is the velocity of the drilling fluid along the outside annulus, and V_2 is the outlet velocity of the nozzles.

The total water passing area of the nozzles is S_T. There are n respective main and assistant nozzles.

$$S_T = n\pi r_1^2 + \mathrm{n}\pi r_2^2 \tag{2}$$

The main waterway area is the product of the bit wall thickness (D-d)/2 and the main waterway width b_1. The area of the assistant waterways is approximately a product of half the wall thickness of the bit (D-d)/4 and the width of the assistant waterways b_2. Therefore, the ratio of the total area of the waterways to the projected area of the bit crown surface can be calculated as follows:

$$S(r_1, r_2) = \frac{nb_1 \dfrac{D-d}{2} + nb_2 \dfrac{D-d}{4}}{\dfrac{\pi}{4}(D^2 - d^2)} \tag{3}$$

The minimum $S(r_1, r_2)$ is taken here as the objective function to increase the projected area of the crown of the bit while satisfying the smooth flow of the water passage system and the normal return of carried cuttings. The above equations can be combined accordingly:

$$\begin{cases} S_{\min}(r_1, r_2) = \dfrac{n(2r_1 + 2)\dfrac{D-d}{2} + n(2r_2 + 2)\dfrac{D-d}{4}}{\dfrac{\pi}{4}(D^2 - d^2)} \\ r_1^2 + r_2^2 = \dfrac{S_T}{n\pi} \\ r_1 - r_2 \geq 0 \\ r_1, r_2 > 0 \end{cases} \tag{4}$$

The ratio of the outer circumference l_D to the inner circumference l_d of the bit can be taken as the grinding ratio l_k:

$$l_k = \frac{l_D}{l_d} = \frac{\pi D - 2n\ （r_1 + 1) - 2n\ （r_2 + 1)}{\pi d - 2n(r_1 + 1)} \tag{5}$$

The minimum value of l_k is the target under the premise of satisfying the normal working life of the bit while reducing the degree of lopsided wear on its inner and outer diameters.

1.3 Calculation of water passage system parameters

The bit used in this study is HQ size, which is often used for geological small-diameter core drilling. The outer diameter of the bit is 96 mm and the inner diameter is 62 mm. The outer diameter of the drill pipe is 89 mm and the hole wall diameter is 97 mm. According to the seafloor core drilling regulations, the upward return velocity range of drilling fluid is 0.75-1.4 m/s and the outlet velocity range of the nozzles is 4-7 m/s [19]. The design value of the return flow velocity is V1=0.75 m/s according to the reverse design principle and under the premise of ensuring the normal return of cuttings; this setting minimizes erosion of the hole wall due to the excessive velocity of the drilling fluid. To prevent repeated grinding of the bit matrix caused by the enrichment of cuttings at the hole bottom, the drilling fluid needs sufficient flow velocity as it exits the nozzles. The nozzle outlet flow velocity is V_2=5 m/s to meet this goal. The total water passing area of the nozzles is S_T=175.3 mm^2 according to Eq. (1). Usually, the number of nozzles in an HQ-size bottom jetting bit is 10, 12, 14, 16, 18 [20, 21]. The structural parameters of the water passage system with different nozzle quantities was determined as shown in Table 1 by solving Eqs. (2)-(5).

Table 1 Structural parameters of bit water system

Nozzle quantity $2n$	Main nozzle radius r_1 (mm)	Width of main waterway b_1 (mm)	Assistant nozzle radius r_2 (mm)	Width of assistant waterway b_1 (mm)	S_{min} (r_1,r_2)	l_k
10	3.0	8.0	3.0	8.0	0.24	1.43
12	2.7	7.4	2.7	7.4	0.27	1.42
14	2.5	7.0	2.5	7.0	0.29	1.39
16	2.3	6.6	2.3	6.6	0.32	1.38
18	2.2	6.4	2.2	6.4	0.35	1.36

As shown in Table 1, an increase in nozzle quantity causes S_{min} (r_1, r_2) to increase; that is, the ratio of the total nozzle area to the crown projection area trends downward. This reduces the effective working area of the bit and is not conducive to its service life. Conversely, the grinding ratio l_k decreases as the nozzle quantity increases, which prevents premature scrap of the bit caused by internal diameter deviations. When the number of nozzles is 10, S_{min} (r_1, r_2) is the smallest and l_k is the largest. When the number of nozzles is 18, S_{min} (r_1, r_2) is the largest and l_k is the smallest. Taking into account the effects of the bit crown projection area and the grinding ratio on service life, the middle value of S_{min} (r_1, r_2) and l_k should be selected when determining the number of nozzles. A 14-nozzle water passage system was designed according to these results.

2 Effects of bit water passage system parameters on flow field at hole bottom

2.1 Bit water passage system model

The waterway height of the impregnated diamond bit directly affects the cooling effect of drilling fluid on the cutting tooth crown of the bit and thus the service life of the bit [22, 23]. The waterway height of the bit is usually equal to its working layer height. On the premise of ensuring that the drilling fluid can normally cool the cutting teeth of the bit, the working layer height of the bit should be increased to the greatest extent possible to increase its service life. As per the bit water passage system parameters presented above, a bit model was established in Solidworks as shown in Figure 4. Considering that the waterway height is limited by the cooling effect of the bottom crown of the bit and the manufacturing process, the waterway height is usually less than or equal to 14 mm, so bit models with *h* of 10 mm, 12 mm, and 14 mm were established [24].

Fig. 4 Bit model diagram

The actual assembly of the drilling tool during the drilling process was incorporated into the model as shown in Figure 5. The model encompasses six parts of the water passage: the hole wall, bit, core lifter case, core lifter, stop ring, and core. Solidworks 5 Boolean subtraction operations were used to secure the fluid domain model, one-seventh of which was used as the display object as shown in Figure 6.

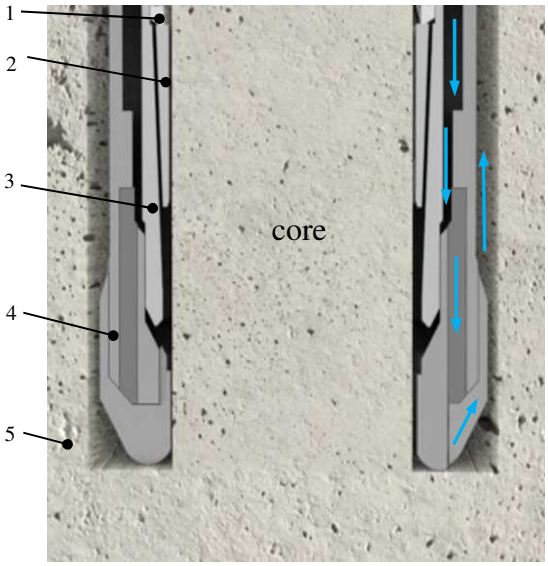

1. Stop ring; 2. Core lifter; 3. Core lifter case;
4. Diamond bit; 5. Hole wall

Fig. 5 Water passage model diagram

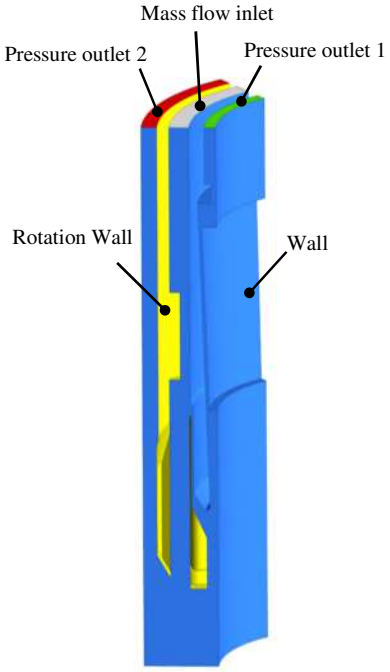

Fig. 6 Water passage simulation model and boundary diagram

2.2 Simulation parameters and boundary setting

In order to facilitate the setting of the boundary conditions of the internal fluid channel and the axial symmetry of the model, one-seventh of the model is used for simulation. The impact of bit rotation on the flow field at the hole bottom was analyzed as shown in Figure 6, where the rotation boundary of the bit is marked in yellow. The rotation speed is 300 rpm and the wall boundary is marked in blue. Seawater was used as the drilling fluid medium with a density of 1.03 kg/m^3 and pump displacement of 80 L/min. The initial conditions for this simulation include a mass flow inlet and two pressure outlets. The mass flow inlet boundary condition is 0.515 kg/s in the annular clearance between the bit and the core lifter case. Two pressure outlets boundary is set to0.89Mpa.The RNG k-epsilon turbulence

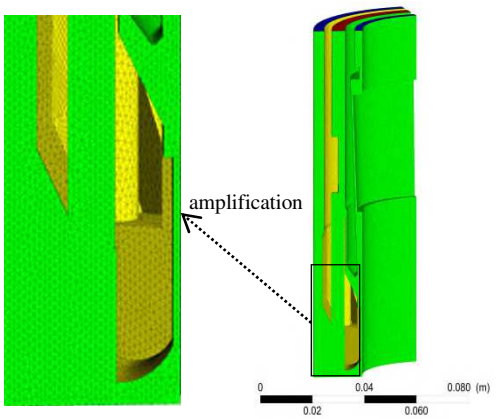

Fig. 7 Octree algorithm generates grid model diagram

model is used for numerical simulation. Using the Improved Mesh Quality of Fluent, the grid with 5 % quality less than 0.5 is increased to more than 0.7, and the grid model diagram is shown in Figure 7.

2.3 Effects of waterway height on drilling fluid velocity at bottom crown of the bit

Fluid simulations were conducted in Fluent software. Velocity nephograms of drilling fluid on the bit crown were obtained with *h* values of 10 mm, 12 mm, and 14 mm (Figure 8). The flow velocity of the crown reflects the cooling effects of the drilling fluid and eddy current size on the return of cuttings, making it an important parameter. In the figure, the red coil is the erosion risk area of drilling fluid to the hole wall, the maximum speed of which is 2.9 m/s when *h*=14 mm. There is a risk of punching the hole wall when drilling in soft strata such as sediments. The black coil in the figure marks the direct injection area of the nozzles. The bit velocities with different waterway heights in this region range from 2.0 to 2.3 m/s. When *h* is 10 mm or 12 mm, there is little difference in the erosion velocity of the hole wall.

The drilling fluid sprayed from each waterway converges to form a vortex. The drilling fluid at the hole bottom is in a state of swirling, which is not conducive to the return of cuttings. The swirling state of the drilling fluid at the hole bottom impedes the return of bottom cuttings, however, when the impregnated diamond bit is used for drilling, a small number of cuttings left at the hole bottom can promote diamond exposure there. A small vortex at the bottom of the borehole is thus conducive to retaining a small number of cuttings to facilitate diamond exposure. As shown in Figure 8, when *h* is 10 mm, the drilling fluid flow velocity of the larger area on the crown is less than 0.2 m/s, which is not conducive to cooling of the bit crown or the return of carried cuttings. When *h* is 12 mm, the bit crown has a small vortex. The eddy current on the crown is significant when *h* is 14 mm, which is not conducive to carrying cuttings in the drilling fluid. The bit waterway is optimal at a height of 12 mm.

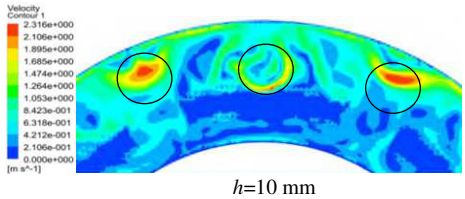

h=10 mm

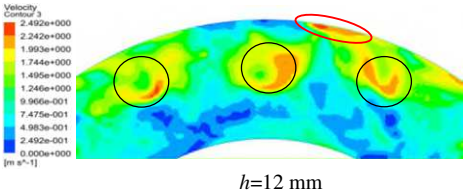

h=12 mm

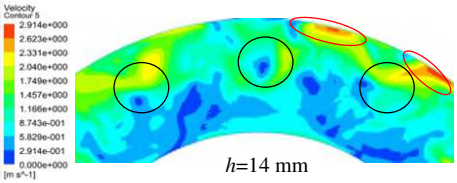

h=14 mm

Fig. 8 Effects of waterway height on crown flow velocity

2.4 Effects of waterway height on drilling fluid intensity of pressure

The main waterway section accurately reflects changes in the drilling fluid and its maximum flow velocity in the core, as well as the flow velocity of the hole wall annulus. Figure 9 shows a pressure nephogram of the drilling fluid at the main waterway section. The pressure gradient is large when the drilling fluid reaches nozzle 1 from the inside annular area. When the drilling fluid reaches the bottom "B", the kinetic energy is converted back into pressure energy. Drilling fluid in the bit and the hole wall annulus "W" water flow area decreases, the pressure reaches its lowest value, then the pressure moves back to the outlet. The bottom pressure region area B increases as waterway height h increases, reaching its maximum at h=14 mm. Without considering the leakage and heat loss at the hole bottom, when h is 10 mm, 12 mm, and 14 mm, the pressure loss is about 17000 pa, 17800 pa, and 184000 pa, respectively. In effect, pressure loss increases as h increases. A waterway height of 10 mm is optimal in terms of minimum pressure loss.

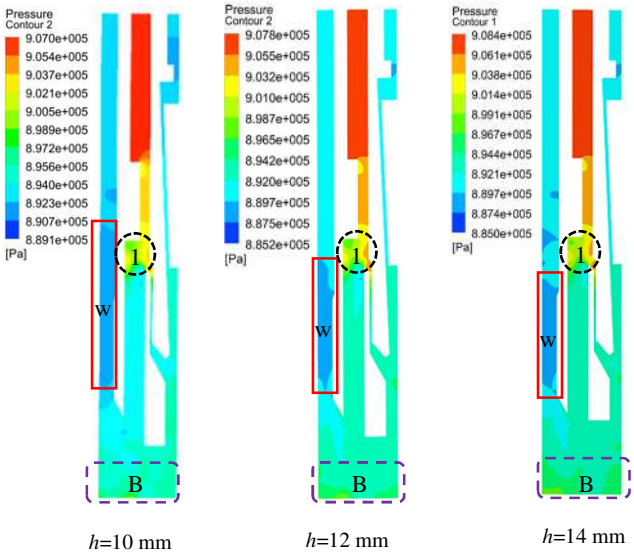

h=10 mm h=12 mm h=14 mm

Fig. 9 Pressure nephogram of main waterway section

2.5 Effects of waterway height on drilling fluid flow velocity

Figure 10 shows the velocity profile of the drilling fluid in the main waterway section. As the drilling fluid reaches the nozzles of the bit, the water area decreases, the pressure energy is converted to potential energy, and the flow velocity reaches its maximum. After the drilling fluid reaches the hole bottom, the flow velocity decreases and then returns along the outside annulus of the hole wall. As shown in Figure 9, when the drilling fluid reaches the outer annulus "W", the pressure energy decreases and the flow velocity increases until stabilizing at about 1 m/s. This satisfies the requirements for seafloor core drilling. The area of the black coil at the bottom increases as waterway

height increases and its flow pattern grows more disordered, which is not conducive to the return of cuttings.

Region “D” is the direct erosion region of drilling fluid to the core. This area's average velocity and maximum velocity are used to identify the erosion degree of drilling fluid to the core. As shown in Figure 10, the decree of scouring by drilling fluid on D decreases as waterway height increases. The core erosion is largest when h=10 mm, and the bottom flow field is excessively disordered when h=14 mm, so the middle height h=12 mm is optimal.

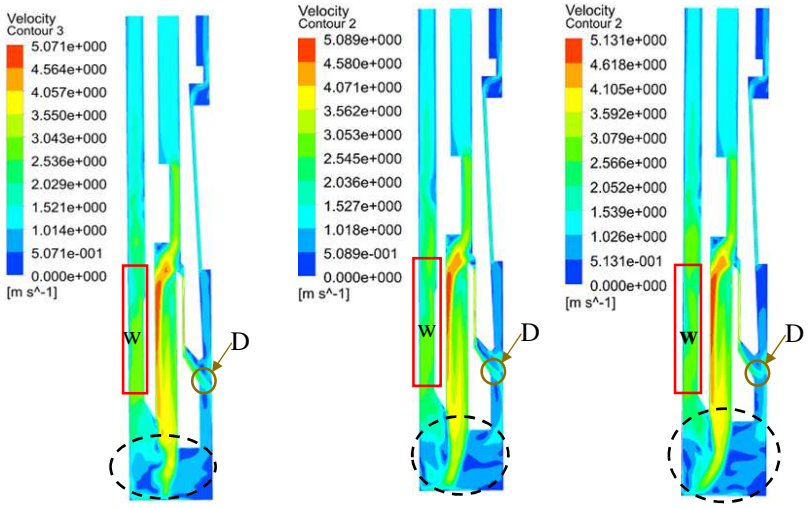

h=10 mm h=12 mm h=14 mm

Fig. 10 Velocity nephogram of main waterway section

3 Effects of drilling parameters on bottom hole flow field

3.1 Effects of pump displacement on flow field at hole bottom

According to the above simulation, about 90% of the drilling fluid returns from the outside annulus, while the remaining 10% returns along the gaps of the stop ring. Therefore, Eq. (6) can be written based on Eq. (1).

$$0.9Q = \frac{60\pi V_1}{4}(D_1^2 - D_2^2)\times 10^{-3} \tag{6}$$

When drilling in soft to medium-hard formations on the seafloor, the return flow velocity of the drilling fluid carrying the cuttings is 0.5-1.4 m/s and the range of the drilling fluid pump displacement Q from Eq. (6) is 40-110 L/min. According to seafloor core drilling regulations, the rotation speed of the bit is 300 rpm. The flow velocity change rule of the drilling fluid pump volume within the calculated range was obtained through Fluent simulation analysis, as shown in Figure 11. When the pump displacement ranges from 40 to 110 L/min, the average flow velocity of outlet 2 increases from 0.34 m/s to 1.35 m/s and the maximum flow velocity of outlet 2 increases from 0.5 m/s to 1.7 m/s. The maximum flow velocity at outlet 1 also increases from 0.43 m/s to 1 m/s. The drilling fluid pump displacement should be controlled within the range of 50-85 L/min. As shown in Figure 12, as the pump displacement increases from 40

L/min to 110 L/min, the pressure loss at the hole bottom increases from 5434 Pa to 23324 Pa.

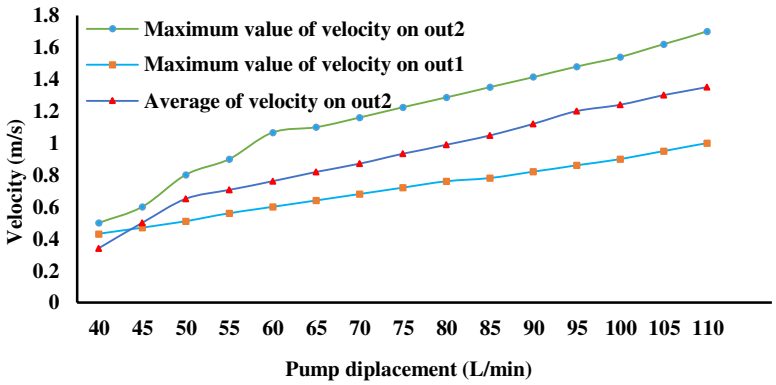

Fig. 11 Effect of pump displacement on outlet velocity of drilling fluid

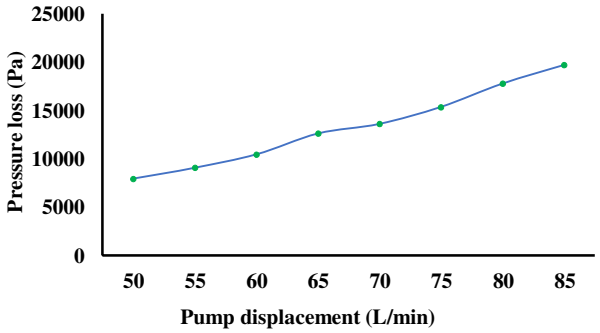

Fig. 12 Effect of pump displacement on pressure loss of bottom hole flow field

3.2 Effects of pump displacement on core surface velocity

The maximum velocity and average velocity of the core surface reflect disturbance to the core due to drilling fluid scouring. Figure 13 shows the variations in maximum velocity and average velocity of drilling fluid affecting the core surface with pump displacement. As the pump displacement increases from 40 L/min to 110 L/min, the maximum velocity on the core surface increases from 0.7 m/s to 3.2 m/s and the average velocity on the core surface increases from 0.45 m/s to 2.6 m/s. The velocity of drilling fluid on the core surface increases with pump displacement, so the disturbance of drilling fluid on the core intensifies. If the core surface velocity of drilling fluid below 1.5 m/s is the safety value for drilling sediment formation, the pump displacement should be 50-65 L/min. When drilling complex formations, the pump displacement and bit rotation speed can be appropriately increased to cool the crown and enhance drilling efficiency.

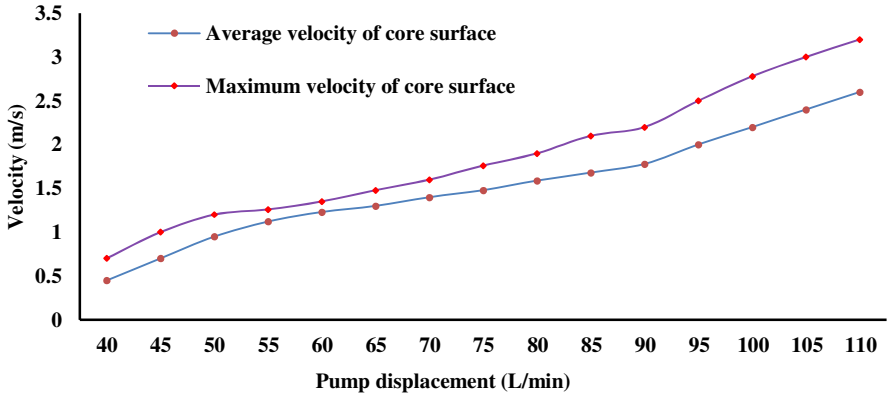

Fig. 13 Effect of pump displacement on core surface velocity

3.3 Effects of bit rotation speed on drilling fluid return velocity

According to the seafloor coring drilling regulations, the rotation speed range of the impregnated diamond bit is 250-700 rpm [19]. An appropriate increase in bit rotation speed can thus enhance drilling efficiency. However, such an increase also increases the amount of cuttings and heat that are generated, and converts the kinetic energy of the bit to that of the drilling fluid. When the maximum pump displacement of drilling fluid is 80 L/min, the velocity of drilling fluid is as shown in Figure 14. When the bit rotation speed increases from 250 rpm to700 rpm, outlet 1 increases from 0.8 m/s to1.41 m/s and outlet 2 from 0.95 m/s to 1.75 m/s. To effectively control the return velocity of drilling fluid, the bit rotation speed should be within the range of 250 rpm to 400 rpm.

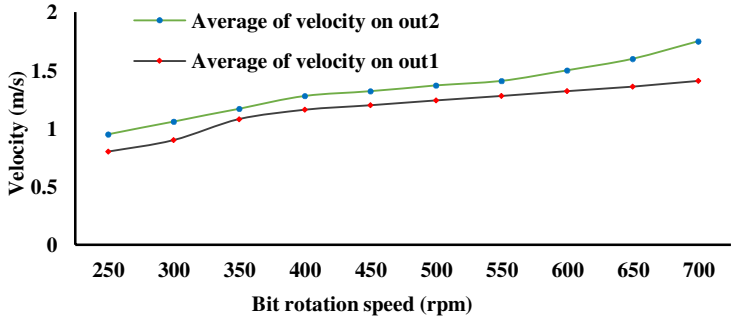

Fig. 14 Effect of bit rotation speed on back flow velocity of drilling fluid

1. Field application

An impregnated diamond bit was fabricated according to the determined water system parameters as shown in Figure 15. The matrix formula is a WC-based matrix formula system, which has good hardness and bending strength and is conducive to the service life of the bit [25]. Sediments mainly dominate the strata within 200 m of the seafloor, so the coarse-grained and low-concentration diamond parameter scheme was selected. This scheme was expected to improve the rock fragmentation efficiency of the bit by increasing the exposed height of the single-grained diamond and

the specific pressure of the bit crown. An appropriate proportion of hard, brittle SiC particles was added to the matrix to promote diamond exposure at a concentration of 15% and an average particle size of 425 μm. The cutting tooth structure is conical, which improves the bit crown pressure and drilling stability. The parameters of the diamond bit are listed in Table 2.

Fig. 15 Finished diamond bit products

Table 2 Diamond bit parameters

Bit size (mm)	Matrix hardness (HRC)	Diamond concentration (vol%)	Diamond size (mesh)
96/62	15	55%	30/35

Field drilling tests were conducted in a mineral resource exploration project in a sea area of China. The seabed sediments in the target area are mainly composed of sediments and unconsolidated flow sand with hard, thin flint layers. A seafloor multi-purpose drilling rig with wireline coring drilling technology was operated throughout the test. The height of the rig is 5.6 m and the bottom size is 2.2 × 2.2 m. The total weight of the seafloor drill is 8.3 tons in air and 6.7 tons in water. The maximum operating water depth is 3500 m. The seafloor drill can carry 25 core pipes simultaneously and has a maximum drilling depth is 62.5 m. Five stations drill over an operating water depth range of 900-1200 m, single hole drilling depth of 62.5 m, and drilling diameter 97 mm. Seawater was used as drilling fluid with drilling pressure of 8-15 kN, rotation speed of 250-400 rpm, drilling fluid pump displacement of 50-80 L/min, and run to a depth of 2.5 m in each iteration. The test is shown in Figure 16 and information regarding drilling operations is given in Table 3.

Table 3 Drilling operation

Station number	Drilling depth (m)	Average drilling efficiency (m/h)	Coring recovery rate (%)
1	62.5	2.8	86.5
2	62.5	3.1	87.6

3	62.5	3.4	83.2
4	62.5	2.9	90.4
5	62.5	3.3	85.4

The total cumulative drilling reached 312.5 m and average drilling efficiency reached 3 m/h. The average coring recovery rate was 86.6%. In drilling process, the bit did not appear to be burnt due to blockage of the water passage system. This suggests that the bit water passage system design is reasonable and can satisfy the real-world requirements for adaptive seafloor drill switching. To this effect, the proposed design may provide a workable reference for water passage systems and drill bit parameter schemes.

1. Seafloor drill deployment operation; 2. Used diamond bits; 3. Core samples

Fig. 16 Field test

5. Conclusions

Seafloor drill operating and formation characteristics were combined in this study to design a water passage system suitable for bottom jetting diamond bits based on the basic theory of multi-objective optimization. Based on fluid dynamics theory and considering the effects of bit rotation on the flow field at the hole bottom, the influence law of the water passage system parameters and drilling parameters of HQ-size bits on the flow field at the hole bottom was determined. The conclusions of this work can be summarized as follows.

(1) Setting the optimization goal of the water passage system as the maximum projection area of the cutting tooth can improve the normal service life of the bit, as grinding length ratio can create lopsided wear between inner and outer diameters.

(2) The flow field of drilling fluid at the hole bottom grows increasingly disordered as the bit waterway height increases, which drives down the efficiency of carrying cuttings and increases pressure loss at the hole bottom.

(3) The optimal bit rotation speed is 250-400 rpm. When drilling in conventional formations, pump displacement control in the range of 50-80 L/min is optimal. When drilling in sediment formations, pump displacement control in the range of 50-65 L/min can reduce drilling fluid damage to the core.

Declarations

Availability of data and materials

The datasets used and/or analysed during the current study are available from the corresponding author on reasonable request.

Competing interests

The authors declare that they have no competing interests.

Funding

This research is supported by the China National Natural Science Foundation (No. 41702390), Open Research Fund Program of Key Laboratory of Metallogenic Prediction of Nonferrous Metals and Geological Environment Monitoring (Central South University), Ministry of Education (2019YSJS15) , National Key R&D Program of China (No. 2017YFC0307501) and Hunan Provincial Natural Science Foundation China (No. 2018JJ3173).

Authors' contributions

J L expounds on the theory on which the paper is based, makes engineering tests, and makes final modifications to the paper. D L has carried on the thesis writing and the numerical simulation. Y establishes a simulation model. F F has guided the numerical simulation of the paper.

Acknowledgments

All authors thank the anonymous reviewers for constructive comments that helped improve this manuscript.

Authors' information

Wang Jialiang, Associate Professor, Master Tutor, Doctor, mainly engaged in marine exploration, diamond broken rock tools teaching and research. ***Qian Dilei*** is a postgraduate student at Hunan University of Science and Technology. ***Sun Yang*** is a postgraduate student at Hunan University of Science and Technology. ***Peng Fenfe***i is a research assistant at Hunan University of Science and Technology.

Reference

[1] Petersen, S., Krätschell, A., Augustin, N., Jamieson, J., Hein, J. R., & Hannington, M. D. (2016). News from the seabed–Geological characteristics and resource potential of deep-sea mineral resources. *Marine Policy*, 70, 175-187.

[2] Arndt, N. T., Fontboté, L., Hedenquist, J. W., Kesler, S. E., Thompson, J. F., & Wood, D. G. (2017). Future global mineral

resources. *Geochemical Perspectives*, 6(1), 1-171.

[3] Merey, Ş. (2019). Evaluation of drilling parameters in gas hydrate exploration wells. *Journal of Petroleum Science and Engineering*, 172, 855-877.

[4]Hanquan Zhang, Qi Chen,Buyan Wan, et al. (2016) Current research and development trends of seabed drill rig.*Journal of Hunan University of Science and Technology*, 1: 1-7.

[5] Sterk, R., & Stein, J. K. (2015). Seabed mineral deposits: an overview of sampling techniques and future developments. *Deep Sea Mining Summit: Aberdeen, Scotland*, 29.

[6] Deshun, L., Yongping, J.,& Yanbu, W. (2014) Review and Development Trends of Deep-sea Mineral Resource Core Sampling Technology and Equipment. *China Mechanical Engineering*,25(23):3255–3265.

[7] Millett, J. M., Wilkins, A. D., Campbell, E., Hole, M. J., Taylor, R. A., Healy, D., & Blischke, A. (2016). The geology of offshore drilling through basalt sequences: Understanding operational complications to improve efficiency. *Marine and Petroleum Geology*, 77, 1177-1192.

[8] Freudenthal, T., & Wefer, G. (2013). Drilling cores on the sea floor with the remote-controlled sea floor drilling rig MeBo.*Geoscientific Instrumentation*, *Methods and Data Systems*, 2(2), 329-337.

[9] Gohl, K., Freudenthal, T., Hillenbrand, C. D., Klages, J., Larter, R., Bickert, T., & Science Team of Expedition PS104. (2017). MeBo70 seabed drilling on a polar continental shelf: operational report and lessons from drilling in the Amundsen Sea Embayment of West Antarctica. *Geochemistry, Geophysics, Geosystems*, 18(11), 4235-4250.

[10] Abimbola, M., Khan, F., & Khakzad, N. (2014). Dynamic safety risk analysis of offshore drilling. *Journal of Loss Prevention in the Process Industries*, 30, 74-85.

[11] Adedigba, S. A., Oloruntobi, O., Khan, F., & Butt, S. (2018). Data-driven dynamic risk analysis of offshore drilling operations. *Journal of Petroleum Science and Engineering*, 165, 444-452.

[12] He, S., Peng, Y., Jin, Y., Wan, B., & Liu, G. (2020). Review and Analysis of Key Techniques in Marine Sediment Sampling. *Chinese Journal of Mechanical Engineering*, 33(1), 1-17.

[13] Wang, J. L., & Zhang, S. H. (2015). A new diamond bit for extra-hard, compact and nonabrasive rock formation. *Journal of Central South University*, 22(4), 1456-1462.

[14] Chen, Y., Liu, Z. Y., & Duan, L. C. (2012). Simulation on hydraulic performance of two kinds of coring diamond bits with different crown. *In Advanced Materials Research*, 497, 350-355. Trans Tech Publications Ltd.

[15] Tan, S., Fang, X., Yang, K., & Duan, L. (2014). A new composite impregnated diamond bit for extra-hard, compact, and nonabrasive rock formation. *International Journal of Refractory Metals and Hard Materials*, 43, 186-192.

[16] Sun, Q. B., Shen, L. N., Yang, G. S., Tian, G. L., Ruan, H. L., & Chen, X. (2020) Design and numerical simulation of multi-layer bit with extra-high matrix. *Coal Geology & Exploration*, 48(03): 225-230.

[17] Gant, A. J., Konyashin, I., Ries, B., McKie, A., Nilen, R. W. N., & Pickles, J. (2018). Wear mechanisms of diamond-containing hardmetals in comparison with diamond-based materials.*International Journal of Refractory Metals and Hard Materials*, 71, 106-114.

[18] Tan, S. C., Duan L. C., Gou , X. D., & Yang, K. H. (2013) Influential factor analysis for lopsided wear of hot-pressed impregnated diamond bit. *Materials Science and Engineering of Powder Metallurgy* , 18(04): 609-614.

[19] Bridges, S., & Robinson, L. (2020). A Practical Handbook for Drilling Fluids Processing. *Gulf Professional Publishing*.

[20] Feng, F., Wan, B. Y., & Huang, X. J. (2016). Structure design and optimization of coring bit for soft sea bottom. *Journal of Machine Design*, 7.

[21] Zheng, M. Z., Li, S. J., Yao, Z., Zhang, A. D., Xu, D. P., & Zhou, J. F. (2020). Core discing characteristics and mitigation approach by a novel developed drill bit in deep rocks. *Journal of Central South University*, 27(10), 2822-2833.

[22] Xu, J., Sheikh, A. H., & Xu, C. (2017). 3-D Finite element modelling of diamond pull-out failure in impregnated diamond bits. *Diamond and related materials*, 71, 1-12.

[23] Franca, L. F. P., Mostofi, M., & Richard, T. (2015). Interface laws for impregnated diamond tools for a given state of wear.

International Journal of Rock Mechanics and Mining Sciences, 73, 184-193.

[24] Liu, Z. Y., Duan, L. C., Zhang, Q. (2011) Simulation on hydraulic performance of two kinds of diamond core bit with different crown. *Diamond & Abrasives Engineering*, 31(06): 43-46+50.

[25] Sun, W., Gao, H., Tan, S., Wang, Z., & Duan, L. (2021). Wear detection of WC-Cu based impregnated diamond bit matrix based on SEM image and deep learning. *International Journal of Refractory Metals and Hard Materials*, 105530.